JOURNAL OF MATERIALS SCIENCE: MATERIALS IN MEDICINE 3 (1992) 59–64

Thermomechanical properties of hyaluronic acid-derived products

S. IANNACE*, L. AMBROSIO*, L. NICOLAIS*, A. RASTRELLI‡, A. PASTORELLO‡
*Department of Materials and Production Engineering and Institute of Composite Materials Technology, University of Naples, Piazzale Tecchio, 80125, Naples, Italy
‡Fidia S.p.A., Via Ponte della Fabbrica 3/A, 35010 Abano Terme, Padova, Italy

The thermomechanical properties of fibres of two hyaluronic acid esters have been evaluated. The materials are found to be significantly different in hydrophilicity, reflected also in variations in mechanical and viscoelastic properties. Both esters show a marked decrease in strength in the swollen state.

1. Introduction

Many implants are designed using pure, homogeneous and biologically inert materials, assuming biocompatibility and biostability are the major requirements for prosthesis [1–5]. However, adequate mechanical properties are often important to the success of an implant, and it is extremely difficult to find materials with both appropriate biological and mechanical properties.

Ideally, an artificial prosthesis temporarily replaces the function of the damaged organ and subsequently induces a regeneration of the natural tissue. This can be achieved by designing the prosthesis using biocompatible materials which degrade slowly after implantation as the body heals itself, and which contain biologically active molecules that stimulate the regenerative tissue growth.

Hyaluronic acid (HA) is a naturally occurring mucopolysaccharide consisting of residues of D-glucuronic acid and *N*-acetyl-D-glucosamine. It is found in cartilage, in eye vitreous humour, skin, umbilical cord and synovial fluid [6]. It seems that proteoglycans and HA play a crucial role during reparative processes influencing the deposition of new synthetic collagen [7, 8].

Through the esterification of carboxyl groups on the hyaluronic acid backbone with therapeutically inactive and active alcohols, it is possible to produce polymers with chemical–physical properties significantly different from those of the HA itself, which can be regarded as a new class of semisynthetic biopolymers. These can be processed leading to a great variety of products such as threads, films, fabrics and sponges, of great interest for example in plastic surgery, wound dressing, orthopaedics, etc.

This paper deals with the thermomechanical characterization of two different esters of HA, in order to investigate the role of the substituent on the properties of these products.

2. Materials and methods

2.1. Hyaluronic acid derivatives

Fibres of the ethyl ester of hyaluronic acid (HYAFF 7, indicated as H7) and the benzyl ester (HYAFF 11, indicated as H11) were supplied by Fidia SpA. Threads with a nominal diameter of 25 μm were obtained by wet spinning starting from a dymethylsulphoxide (DMSO) solution of both esters as described in [9].

2.1.1. Thermal analysis

Calorimetric analyses were performed using a Mettler DSC 30 differential scanning calorimeter model TA300 at a heating rate of 10 °C min^{-1} in a nitrogen atmosphere. Thermogravimetric data were obtained by means of a TGA Du Pont model TA2100 at a heating rate of 10 °C min^{-1} in a nitrogen atmosphere.

2.1.2. Static and dynamic mechanical analysis

The static mechanical properties of the samples were studied by using an Instron instrument at room temperature. Cardboard rectangular tabs with gauge length 30 mm were prepared as sample holders for the fibres. These tabs allowed for easier and consistent alignment of the fibre samples in the Instron grips. Sample fibres were tested on the Instron at a strain rate of 0.3 min^{-1} following ASTM D3822-22.

The mechanical properties of the hyaluronic acid ester fibres were analysed using a Weibull distribution technique. Dynamic mechanical analyses of the dry fibres were performed in the tensile mode on a Dynastat (Imass) instrument. The temperature was controlled by the Dynatherm within 0.1 °C.

2.1.3. Hydrolysis of fibres

The fibres of HYAFF 7 were exposed to the following buffer solution and maintained at 37 °C for several weeks.

0022–2461/92 $03.00 + .12

(a) Potassium acid phthalate buffer (0.005 M, pH = 4.01);

(b) potassium phosphate monobasic–sodium phosphate dibasic buffer (pH = 7.04);

(c) tris(hydoxymethyl) amino methane buffer (pH = 10.4).

Upon removal from the bath, the fibres were rinsed and dried under vacuum at 25 °C for 24 h, then tested under tension to analyse the mechanical properties.

3. Results and discussion

Fig. 1 reports the DSC curves for the two different esters of the hyaluronic acid. Three different peaks are noted: the first endothermic effect is related to a loss of water from the materials; the others are connected with a complex phenomenon of thermal modification that leads, in conclusion, to the formation of carbon. After a further heating of the dehydrated samples to 180 °C, the DSC curves do not show any peak confirming the absence of water (see Fig. 2).

The second slightly noticeable endotherm which appears in Fig. 1 at ~ 240 °C is associated with the beginning of the dehydration process, and is followed by a pronounced endopeak that coincides with vigorous chemical modifications such as cleavage of bonds and degradation [10]. Thermogravimetric analyses confirm these results (see Fig. 3); from 25 to 100 °C the loss of weight is related to the change in water content; at 225 °C a thermal decomposition begins, characterized by an intensive loss of mass upto ~ 280 °C. The followed region features a deceleration of the loss of

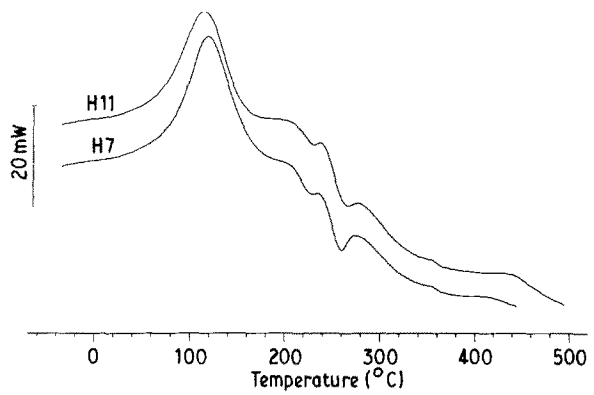

Figure 1 DSC thermograms of H7 and H11. Heating rate, 10 °C min^{-1} (nitrogen atmosphere).

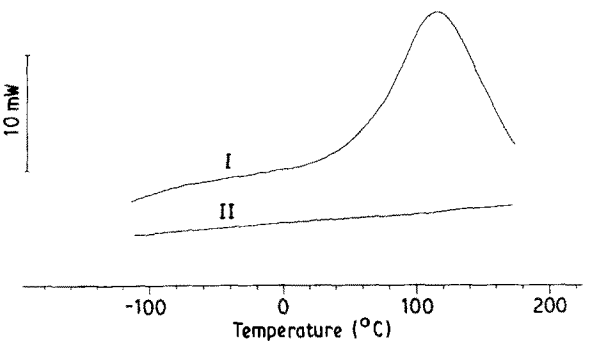

Figure 2 DSC thermograms for H7. Note the absence of the endothermal peak in the second scan (II).

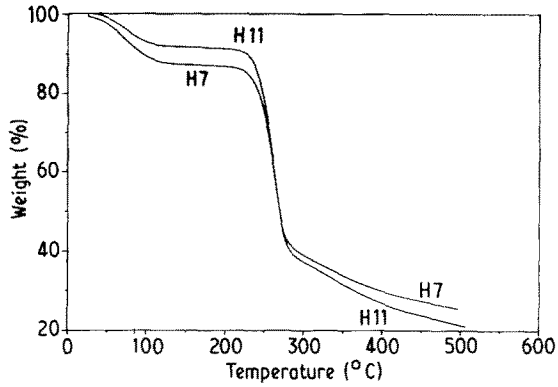

Figure 3 TGA curves for the two hyaluronic acid derivatives. Maximum rate of the mass loss is ~ 265 °C.

mass. The maximum rate of mass loss corresponds to ~ 265 °C. Within 200 to ~ 300 °C, the mass loss reaches ~ 54% for H11 and ~ 48% for H7.

Without entering into detail of the chemical reaction mechanism which generates this behaviour, our analysis is restricted to a description of the observed phenomena. The similar thermal behaviour of the two esters, as shown in Figs 1 and 3, can be associated with the same polysaccharide structure of the two materials. Usually, thermal degradation of polysaccharides results in the formation of volatile products, tars and coke residue. A great number of reactions are involved in the destruction of the polymer. The presence of many hydroxyl groups in esters of hyaluronic acid (EHA), their spatial arrangement and low thermal stability, provide conditions for the course of dehydration reactions in the pyrolysis of the EHA.

TGA measurement shows that the water gain is ~ 13% for fibres of H7 and ~ 10% for H11. From theoretical calculation, it follows that three molecules of water are bonded at each repeating unit of H7, and 2.4 water molecules for H11. These values are calculated by the simple relationship

$$n_{H_2O} = \text{PM(EHA)\% WG/18}$$

where n_{H_2O} is the number of water molecules for each repeating unit, PM(EHA) the molecular weight of the specific EHA (H7 or H11) and % WG the percentage water gain. The different values of n_{H_2O} for the two esters are due to their different microstructures.

During the spinning process, there is formation of hydrophobic and hydrophilic microdomains; the size and structure of these microdomains, influence the different absorption of water at room condition.

In general, the EHA fibres can be considered to be constituted of macromolecules, with packing order varying from point to point within the fibres. In a region of high packing order, the molecules are held together by hydrogen bond formation between hydroxyl groups. In some regions, where there is a smaller order in the structure, the number of hydroxyl groups involved in hydrogen bondings with an adjacent EHA molecule decreases, so in disordered regions a large number of EHA hydroxyls are not hydrogen bonded and can be responsible for the water absorption. The presence of water can lead to a swelling of

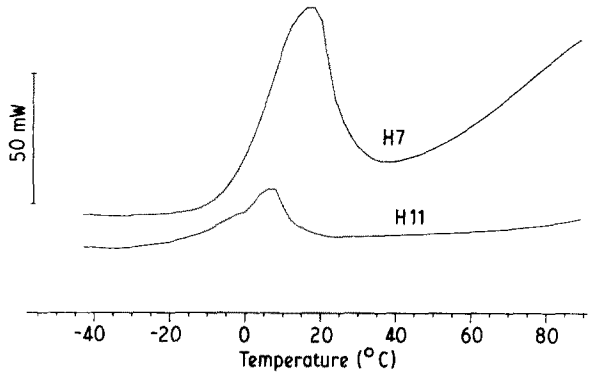

Figure 4 DSC thermograms of the swollen H7 and H11. Note the endothermal peak at ~ 0 °C.

the structure which breaks hydrogen bondings between EHA molecules, so that the number of active sorption centers increases as more water is absorbed. At limit, at high humidity conditions, additional water can be added as condensed water in the swollen structure.

This hypothesis has been verified for the swollen samples by means of thermal analysis. The DSC curves of the swollen samples (see Fig. 4) show the presence of an endothermic peak around 0 °C that is absent for the dry samples. On the basis of the assumption that water absorbed by hydrogen bonding will not freeze, the endothermic peak confirms the presence of free water in the structure. A water gain of ~ 50% was observed for the benzyl and ~ 370% for the ethyl ester; this data also reflects the different microdomains induced from the two components.

3.1. Static and dynamic mechanical properties

These properties are also influenced by the presence of water in the structure of EHA. Fig. 5a and b show the stress–strain curves of the dry and swollen fibres. First of all, the strength of the swollen sample, as expected, is much lower than that of the dry sample for both H7 and H11. The swollen materials also show increasing elongation at break; these trends are observed for the hydrogels in general. Moreover, the effect of the ethyl substituent of the EHA is reflected in the further lowering of the strength.

The stress–strain relations of H7 are also very different from H11. In fact, the dry benzylic esters show a yield point followed by a plastic elongation that is absent in the H7 curve. Moreover, the benzylic substituent causes an increase of the elastic modulus that is also confirmed by dynamic-mechanical data.

The swollen samples of H11 show a yield point followed by a great elongation with a higher elastic modulus than the samples of the swollen H7. In this case, the trend is related to the different amount of water absorbed from the two materials.

The viscoelastic properties of these two EHAs are also influenced by the substituents. Fig. 6 reports the elastic moduli of H7 against frequency at five different temperatures. Before starting each test, the temperature was held for 1 min. An increase of M' (dynamic storage modulus) was observed heating the sample

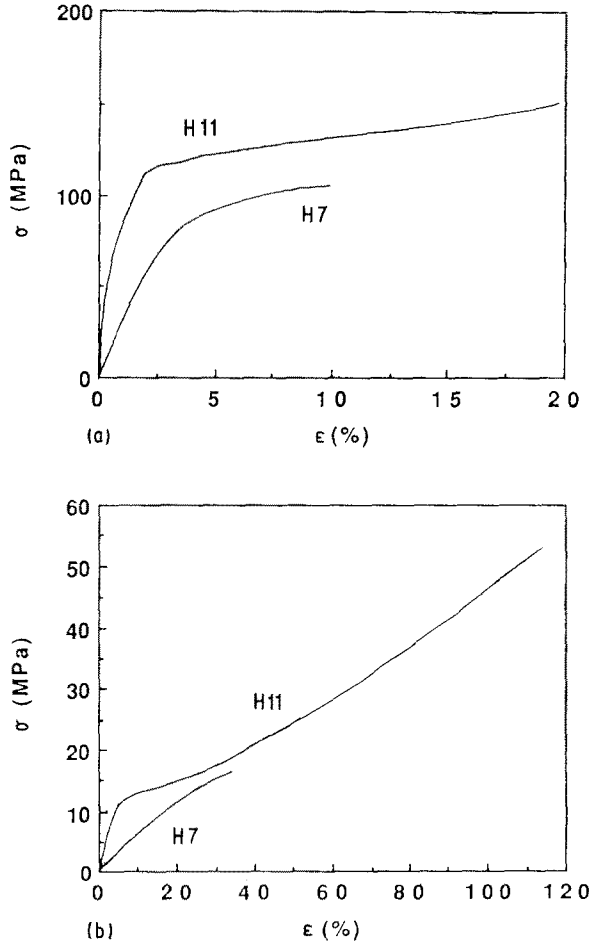

Figure 5 Stress–strain curves of (a) H7 and H11 at room temperature; (b) swollen H7 and H11.

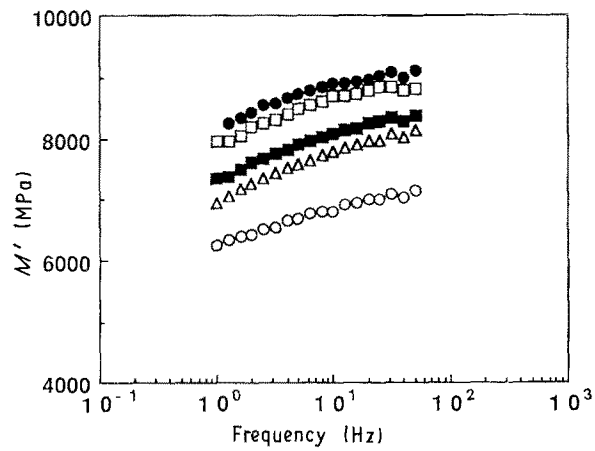

Figure 6 Storage modulus of H7. ○, 22; ●, 37; □, 77; ■, 117; △, 140 °C.

from 22 to 37 °C, followed by a light decrease as the temperature increases above 37 °C. The reduction of M' against temperature is connected with the higher dissipation of the molecules at higher temperature. The initial increase of M' from 22 to 37 °C can be related to the loss of water from the structure, reflected in an increase in stiffness and rigidity. From another point of view, the water cannot permit the formation of hydrogen bonds between the molecules of EHA, and thus the molecules store less energy. A comparison of the two different esters is shown in Figs 7 and 8 which

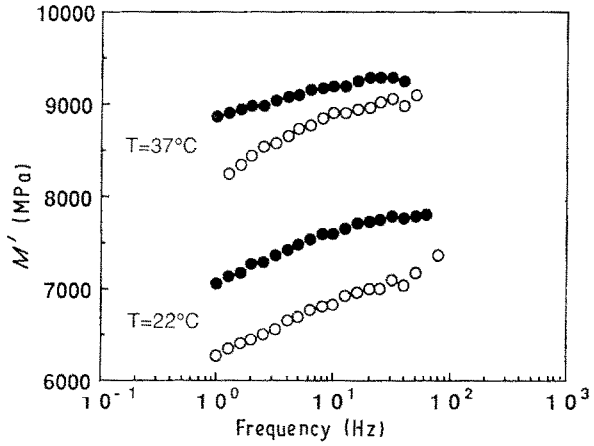

Figure 7 Storage modulus of (○) H7 and (●) H11 at 22 and 37 °C.

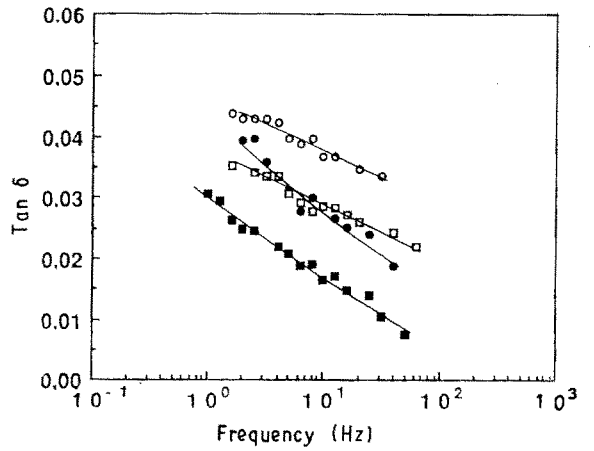

Figure 8 Tan δ of H7 and H11 at 22 and 37 °C. Note the different trends at the two temperatures. H7: ○, 22; ●, 37 °C; H11: □, 22; ■, 37 °C.

give the storage and the loss modulus at room temperature and at 37 °C. According to the static–mechanical data, the benzylic substituents lead to an increase in elasticity for each temperature, as shown by the values of M' and tan δ.

The presence of water at room temperature influences the trend of tan δ which becomes less sensitive with frequency. In fact, at 37 °C the slope of tan δ curve is more pronounced than at 22 °C for both materials.

3.2. Analysis of strength with a Weibull distribution function

To better characterize the fibres, a statistical treatment of the tensile strength has been performed. For the statistical study of single fibre, a key concept is to consider a fibre of length 1, divided into n links (not known in advance) and where the strength of each link depends on the natural flaw, so that the fibre strength is that of the link which has the more severe flaw. It can be assumed that the probability, W_1, of survival of a link at a stress, σ, may be expressed as

$$W_1(\sigma) = \exp[-h(\sigma)] \quad (1)$$

where the function $h(\sigma)$ depends on the unknown distribution of flaws in the fibre links and cannot be predicted. Weibull [11] has proposed a suitable function

$$h(\sigma) = [(\sigma - \sigma_S)/\sigma_o]^\alpha \quad (2)$$

where σ_o, α and σ_S are adjustable parameters. The probability of survival of a fibre composed of n links is given, obviously, by the nth power of Equation (1). Combining Equations (1) and (2), we obtain

$$W(\sigma) = W_1(\sigma)^n = \exp\{-n[(\sigma - \sigma_S)/\sigma_o]^\alpha\} \quad (3)$$

where $W(\sigma)$ is the probability of survival of a fibre at stress σ. Therefore the probability of breaking of a fibre before reaching a stress σ is obtained as the cumulative distribution function

$$F(\sigma) = 1 - W(\sigma) = 1 - \exp\{-[(\sigma - \sigma_S)/\beta]^\alpha\} \quad (4)$$

where n is incorporated in the new adjustable parameter β.

Fig. 9 reports the Weibull distributions for the two esters. The two parameters β and α have been calculated maximizing the likelihood function. The means of the two distributions are different, and there is also a small difference between the shape of the two functions, as confirmed by the values of the parameter β and α reported in Table I. The best correlations with the experimental data were obtained with $\sigma_S = 0$ for both esters.

The experimental data are compared with the theoretical curves in Fig. 10, obtained taking the lnln transform of $F(\sigma)$ as follows:

$$\text{lnln}[1 - F(\sigma)]^{-1} = \alpha \ln \sigma - \alpha \ln \beta \quad (5)$$

In this figure, the data are reported as lnln $(1 - p_i)^{-1}$against $\ln \sigma_i$ where p_i is connected to the experimental cumulative distribution and is calculated as $p_i = (i/n + 1)$ (n is the total number of experimental

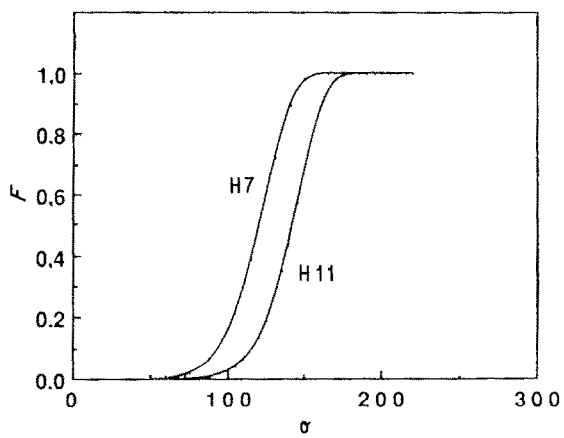

Figure 9 Weibull cumulative distribution of H7 and H11.

TABLE I Weibull parameters for H7 and H11

	HYAFF 7	HYAFF 11
β(σ)–(MPa)	127.9	147.7
α(σ)	9.37	8.61

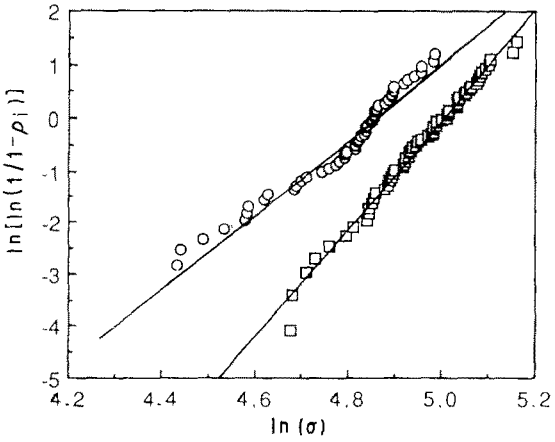

Figure 10 Comparison between experimental data (point symbols) and Weibull function (straight line). ○, H7; □, H11.

values of σ_i) and σ_i is the statistical order (the arrangement of all the data in increasing order). It can be seen that there is a good correlation between the experimental and theoretical values. Moreover, the good alignment of the data on the straight line excludes the presence of a bimodal distribution, and reflects a homogeneous structure of the fibres with a defect of only one type. Other authors have shown how the structure of some fibrous materials influence the statistical distribution of the tensile strength, often presenting multimodal functions [12].

3.3. Hydrolysis of fibres

It is well known that polysaccharides such as hyaluronic acid show good stability under certain conditions, but can undergo degradation by a variety of chemical and physical processes. The most common manifestation of deterioration is a decrease in the mechanical properties of the material. Figs 11–13 give the mechanical characterization against time for the three different pH values. The results are normalized with respect to the values of the untreated materials.

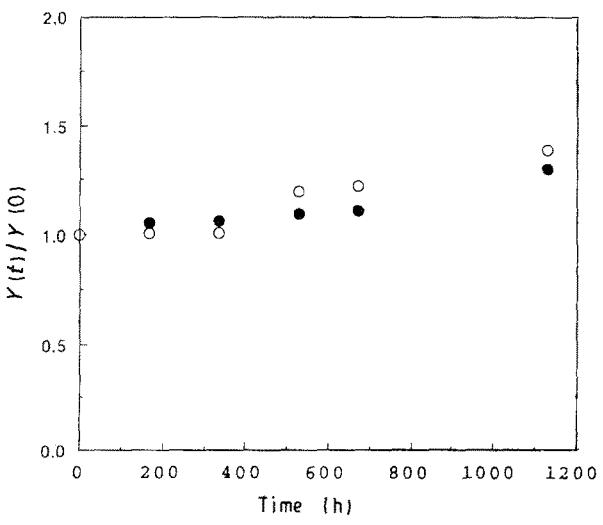

Figure 11 Normalized σ (○) and ε (●) against time for pH = 4.02.

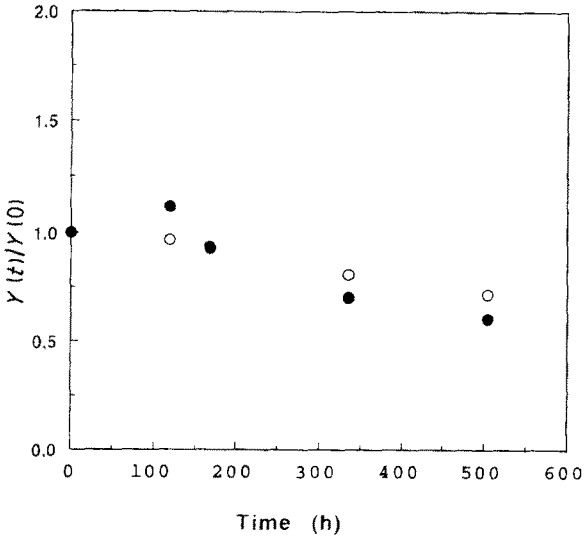

Figure 12 Normalized σ (○) and ε (●) against time for pH = 7.04.

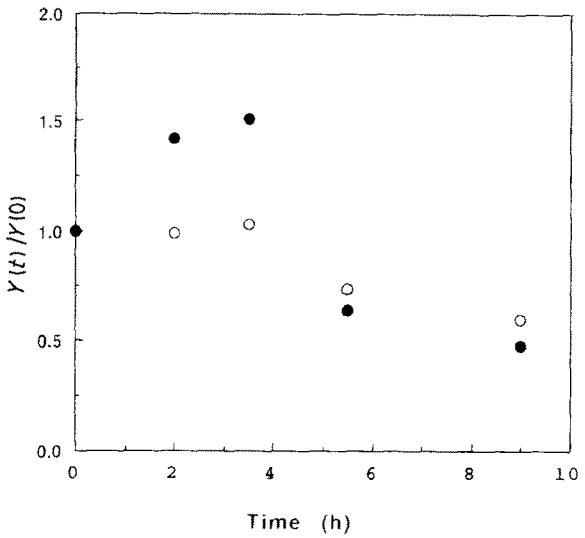

Figure 13 Normalized σ (○) and ε (●) against time for pH = 10.

While the pH = 4.01 buffer solution (see Fig. 11) gives a slight increase of the ultimate properties of the ethyl ester, for the other conditions a reduction of strength and strain at break is evident with time (Figs 12 and 13). At pH = 10.4, a fast alkaline hydrolysis of the molecules is present; after only 5 h a decrease in strength of about 25% can be noted due to the possible saponification of the esters that became soluble in water. The initial increase of the elongation at break against time, shown in Figs 12 and 13, may be due to an initial plasticization of the material.

4. Conclusions

The thermal properties of the two hyaluronic acid esters are connected to the polysaccharide structure of the molecules, and are poorly influenced by the substituents. The two semi-synthetic materials investigated show good mechanical properties in the dry state. In contrast, the strong decrease in mechanical strength for the swollen materials may restrict the

possibility of using these materials in biomedical applications where a contact between water and material, coupled with good mechanical properties, are necessary. Static and dynamic mechanical properties have shown that the fundamental role of the substituent on the microstructure is to modulate the hydrophobic and hydrophilic microdomains which are responsible for the interactions with water molecules and hence of the variation of the mechanical properties.

References

1. J. R. PARSON, H. ALEXANDER and A. E. WEISS, in "Biocompatibility Polymers, Metals and Composites", edited by M. Szycher (Technomic, Lancaster, Pennsylvania, 1963) Ch. 38.
2. D. K. GILDING, in "Biocompatibility of Clinical Implant Materials", edited by D. F. Williams (CRC, Boca Raton, Florida, 1982) Ch. 9.
3. R. L. KRONENTAL and Z. OSER, (eds) in "Polymers in Medicine and Surgery" (Plenum, New York, 1975) p. 119.
4. S. J. HUANG, in "Encyclopaedia of Polymer Science and Engineering", edited by H. F. Mark, N. Bikales, C. G. Overberg and Menges, Vol. 2, 2nd edn (Wileys, New York, 1985) p. 220.
5. P. JARRETT, S. J. HUANG, J. P. BELL, J. A. CAMERON and C. BENEDICT, *Org. Coat. Plast. Chem.* **47** (1982) 45.
6. W. W. GRASSLEY, *Adv. Polym. Sci.* **16** (1974) 3.
7. R. MONSANO, L. ORCI and P. VASSALLI, *J. Cell. Biol.* **97** (1983) 1648.
8. C. J. DOILLON, F. H. SILVER and R. A. BERG, *Biomater.* **8** (1987) 195.
9. F. DELLA VALLE and A. ROMEO, European Patent Application EP 216453, April 1987.
10. A. A. KONKIN, "Production of Cellulose Based Carbon Fibrous Materials" in Handbook of Composites, Vol. 1. Series editors A. Kelly, Yu. N. Rabotnov, Elsevier, Amsterdam, 1985.
11. W. WEIBULL, *J. Appl. Mech.* **18** (1951) 293.
12. L. V. KOMPANIETS, V. V. POTAPOV, G. A. GRIGORIAN, E. V. PRUT and N. S. ENIKOLOPIAN, *Polym. Compos.* **6** (1985) 54.
13. A. S. WATSON and R. L. SMITH, *J. Mater. Sci.* **20** (1985) 3260.

Received 6 August
and accepted 16 August 1990